Journal of Structural Geology 30 (2008) 1507–1519

Contents lists available at ScienceDirect

Journal of Structural Geology

journal homepage: www.elsevier.com/locate/jsg

Influence of a transverse basement fault on along-strike variations in the geometry of an inverted normal fault: Case study of the Mosha Fault, Central Alborz Range, Iran

A. Yassaghi*, S. Madanipour

Department of Geology, Tarbiat Modares University, P.O. Box 14115-175, Tehran, Iran

ARTICLE INFO

Article history:
Received 23 February 2008
Received in revised form 12 August 2008
Accepted 23 August 2008
Available online 13 September 2008

Keywords:
Central Alborz
Inversion tectonics
Transverse basement fault
Footwall shortcut thrusts
Hanging-wall break-back thrusts

ABSTRACT

Inverted normal faults show variations in structural geometry from footwall shortcut thrusts to hanging-wall break-back thrusts. In the present study, we evaluated along-strike variations in the geometry of the Mosha Fault, Central Alborz Range, Iran. Detailed structural mapping within the Taleqan Mountains revealed that the Mosha Fault in the eastern part of the study area is associated with a large, basement-cored hanging-wall anticline thrust over Tertiary rocks that occur as a syncline or cut by footwall shortcut thrusts. In the western part of the study area, however, the hanging wall consists of break-back thrust sheets of Paleozoic–Mesozoic rocks. These thrust sheets occur as a duplex system and have allochthonous masses gravitationally emplaced in the foothills of the Taleqan Mountains. Curved fold axial traces and scattered intrusive bodies are observed in the Valian Valley area, where the Mosha Fault is displaced across a transverse basement fault. This basement fault controlled along-strike variations in the geometry of the Mosha Fault during its evolution from a basin-bounding fault to an inverted normal fault. Inversion of the fault in the eastern part of the study area, where the fault is relatively steep, involved basement rocks; in the western part of the study area, where the fault is relatively shallowly dipping, deformation in the hanging wall is accommodated by thin-skinned break-back thrust sheets.

© 2008 Elsevier Ltd. All rights reserved.

1. Introduction

Inversion tectonics, a common process in regions of collisional orogenesis, involves the reactivation of major extension-related normal faults as reverse faults (Powell, 1989; Williams et al., 1989). In regions of inversion tectonics, the geometry of the original extensional faults influences the geometry of the reactivated normal faults (Etheridge, 1986; McClay and Buchanan, 1992). In addition, deformation during inversion is potentially accommodated in the footwall and/or hanging wall of inverted normal faults (Coward, 1994) (Fig. 1).

Inversion of a high-angle normal fault causes deformation transfer to the fault footwall via shortcut thrusts (Buchanan and McClay, 1991; Konstantinovskaya et al., 2007), as commonly observed in both experimental and natural inverted high-angle normal faults (Fig. 1a) (Brooks et al., 1983; Koopman et al., 1987; Buchanan and McClay, 1991; Quintana et al., 2006; Ventisette et al., 2006). Basement rocks are involved in the reactivation of high-angle extensional faults (Mitra and Mount, 1998; Stockmal et al., 2004), and fold structures in cover rocks are cored by basement and bounded by inverted normal faults (Tavarnelli et al., 2004). Gently dipping extensional faults are readily reactivated, but may be associated with hanging-wall break-back thrusts (Fig. 1b), especially in regions of oblique inversion (Hayward and Graham, 1989; Coward, 1994; Butler et al., 2006; Saura and Teixell, 2006). Along-strike variations in the dip of the original normal faults are mainly controlled by transverse basement faults (Gillcrist et al., 1987; Tavarnelli et al., 2004; Butler et al., 2006). These transverse faults are also associated with anomalously high heat flow, making them loci for volcanic activity (Butler et al., 2006).

The Alborz Range, located in the central Alpine Himalayan orogenic system, marks the southern margin of the Caspian Sea (Fig. 2). The Mosha Fault is the most prominent structure in the southern part of the Central Alborz, across which Precambrian, Paleozoic, and Mesozoic rocks are thrust to the south over Eocene rocks within frontal Alborz folds (Fig. 2). The majority of studies on the Mosha Fault (e.g., Allen et al., 2003; Ashtari et al., 2005) have focused on the eastern portion of the fault (east of 51°40′ E) where the fault strikes approximately E–W. Zanchi et al. (2006) reported the inversion of the Mosha Fault in the Shahrestank, describing several grabens bounded by inverted normal faults. In addition, Moinabadi and Yassaghi (2007) documented the involvement of

* Corresponding author. Tel.: +98 21 8288 3406; fax: +98 21 8800 9730.
E-mail address: yassaghi@modares.ac.ir (A. Yassaghi).

0191-8141/$ – see front matter © 2008 Elsevier Ltd. All rights reserved.
doi:10.1016/j.jsg.2008.08.006

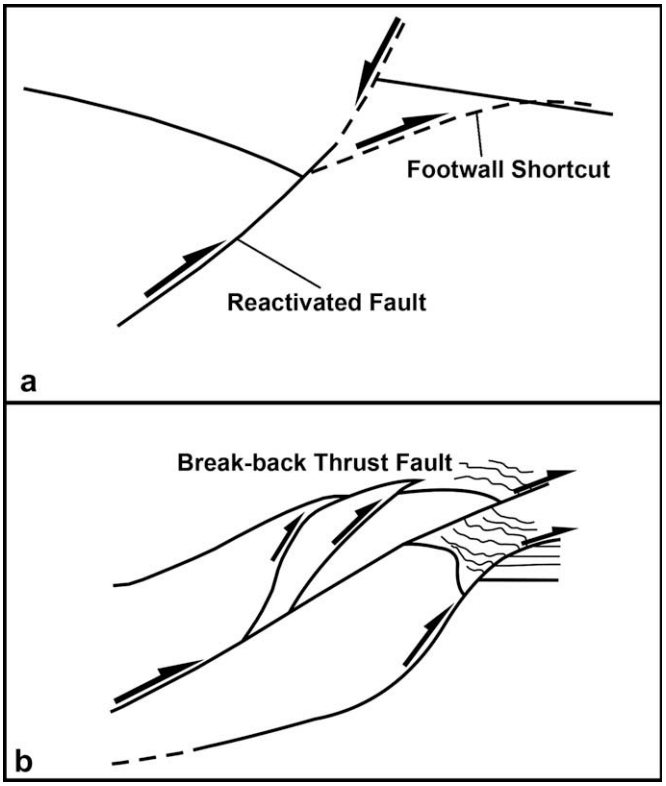

Fig. 1. (a) Geometry of a high-angle inverted normal fault associated with a footwall shortcut thrust. (b) Accommodation of thin-skinned break-back thrusts in the hanging wall of a reactivated low-angle normal fault during inversion tectonics, after Coward (1994).

basement during reactivation of the Mosha Fault in the Nesa area, west of the Shahrestanak area.

The western portion of the Mosha Fault, the subject of the present study, lies along the southern flank of the Taleqan Mountains (west of 51° E; Fig. 2), where it has a general WNW–ESE strike and variable along-strike geometry. This paper presents a detailed analysis of the westernmost Mosha Fault, Taleqan Mountains, with the aim of testing a proposed inversion model in which the fault acted as a major basin-bounding fault in the Central Alborz Range until the Late Mesozoic, and has since been reactivated (Yassaghi, 2001; Zanchi et al., 2006; Moinabadi and Yassaghi, 2007). We also undertook detailed structural mapping of the fault zone and associated structures (Fig. 3) to

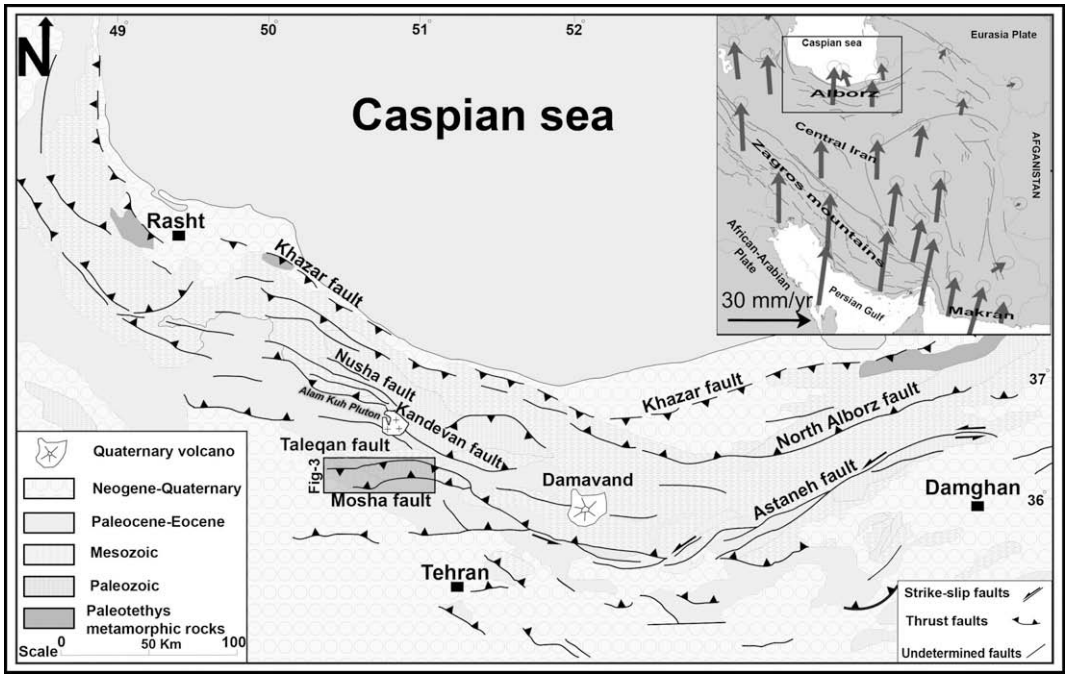

Fig. 2. Structural map of the Alborz Range. The location of the Taleqan Mountains (present study area, see Fig. 3) is indicated by the rectangle. The inset figure is a fault map of Iran (from Berberian and Yeats, 1999); arrows show GPS velocities of points in Iran relative to stable Eurasia (from Vernant et al., 2004). Note the location of the Alam Kuh intrusive body.

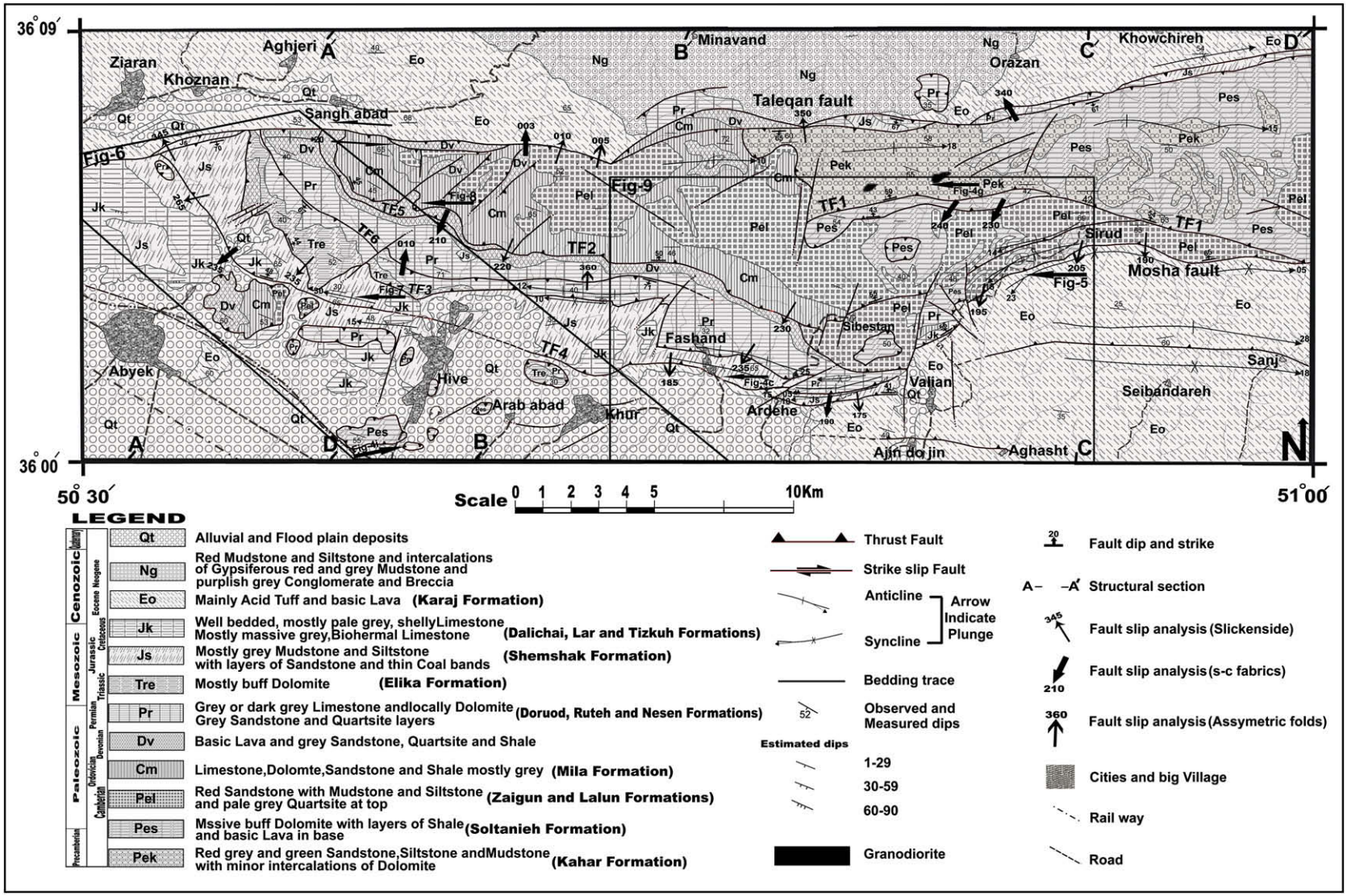

Fig. 3. Structural map of the Taleqan Mountains. Rectangles show the locations of Figs. 6 and 9; arrows indicate the locations shown in other figures. Structural sections (A–A′ to D–D′) are presented in Fig. 4.

assess the role of a transverse basement fault in controlling along-strike variations in the geometry of the Mosha Fault.

2. Geological setting

The Alborz Mountains represent a composite orogenic belt that underwent shortening and uplift during the Tertiary (Alavi, 1996). Almost all of the shortening was accommodated by movement along north- and south-dipping reverse faults, which, along with associated structures (i.e., hanging-wall anticlines and footwall synclines), are the main structures within the Alborz Range. The reverse faults are largely south-directed in the southern part of the range, and north-directed and relatively steeply dipping in the northern part (Fig. 2).

The strikes of major reverse faults within the Alborz Range vary from NW–SE in western areas to NE–SW in eastern areas (Fig. 2), with faults in the central part of the range showing a progressive transition in strike between NW–SE and E–W (e.g., Berberian et al., 1993). From north to south, these faults of the central area are the Khazar, North Alborz, Nusha, Kandevan, Mosha, and North Tehran faults (Fig. 2) (e.g., Vahdati Daneshmand, 2001). Most of these faults have controlled sedimentary deposition in the region since the Early Mesozoic. The Mosha Fault, one of the most prominent reverse faults in the Central Alborz, separates Paleozoic–Mesozoic rocks in the hanging wall from Tertiary rocks in the footwall.

The Taleqan Mountains are located in the southern part of the Central Alborz Range, northwest of Tehran. The present study area is bounded by the Taleqan Fault in the north and the Mosha Fault in the south (Figs. 2, 3). The Late Proterozoic Kahar Formation is the oldest known formation within the Alborz Range; unequivocally Precambrian metamorphic basement has yet to be reported. The Kahar Formation, deposited in a tidal environment, is conformably overlain by a Cambrian–Triassic platform succession (Lasemi, 2000). This Proterozoic–Triassic sedimentary succession is locally up to 6 km thick (Allen et al., 2003).

Sediments were deposited over much of the Central Alborz during the Early Jurassic, including coal-bearing deltaic clastic sediments of the Rhaetic–Liassic Shemshak Formation. Middle Jurassic–Early Cretaceous marine carbonates and clastic sediments are overlain by Late Cretaceous carbonates, basalts, and andesites were extruded across large parts of the Alborz (Allen et al., 2003). The Cretaceous is generally characterized by pelagic carbonates that progressively extend over the Late Jurassic carbonates. Elsewhere in the Alborz Range, conglomerate of the Fajan Formation was deposited during the Paleocene, overlain by interbedded andesitic volcanics and clastic rocks of the Eocene Karaj Formation, principally exposed in the southern Alborz where the formation is locally 5 km thick (Allen et al., 2003).

Few Oligocene deposits are known from the Alborz, although terrestrial red beds of this age (Lower Red Formation) occur to the south, in central Iran. Miocene fluvial and lacustrine clastic rocks occur in intermontane basins within the Alborz, within the cores of footwall synclines linked with major thrusts such as the Mosha Fault. The Cenozoic succession within and adjacent to the Alborz generally shows a coarsening-upward trend, suggesting increasing subaerial relief over time, consistent with evidence for ongoing compressional deformation along major thrust faults such as the Mosha Fault (Stöcklin, 1974; Alavi, 1996).

3. Geometry of the major structures within the Taleqan Mountains

3.1. Mosha Fault

The Mosha Fault, first described by Dellenbach (1964), is a major high-angle (dip of 55°) reverse fault that extends more than 200 km throughout the Central Alborz. Its strike changes from WNW–ESE in the west of the range to NE–SW in central parts and E–W in eastern areas. This study concentrates on the structural geometry of the western part of the Mosha Fault, in the Taleqan Mountains (Figs. 2, 3). This section of the fault was also studied by Guest et al. (2006) in a regional-scale study of the Central Alborz Range.

In the eastern part of the present study area, the Mosha Fault dips relatively steeply (60°) to the north (Fig. 3). The hanging wall contains the prominent Precambrian Kahar Anticline (see section C–C′ in Figs. 3, 4), while the footwall contains a large syncline of the Eocene Karaj Formation. The hanging-wall anticline and footwall syncline are the main regional structures associated with the fault in the eastern part of the study area (Fig. 5a,b). The fault zone in this part of the study area is up to 100 m thick, and contains semi-ductile minor structures such as asymmetric folds (Fig. 5c). An analysis of minor-fold asymmetry data reveals SW-directed displacement along the fault (Fig. 5d). The fault strikes E–W until the Valian Valley area, where it is displaced to the south across a N–S-striking transverse fault (Fig. 3).

In the western part of the study area, west of the Valian Valley area, the Mosha Fault dips at less than 50° (compare sections B–B′ and C–C′ in Fig. 4d and e, respectively). Here, the fault is mapped to the northwest of Khur Village; further to the west it is overlain by Quaternary deposits (Fig. 3). In this part of the study area, the hanging wall comprises a series of thin-skinned thrust sheets (TF2 to TF4 in Figs. 3, 4a) of Paleozoic–Mesozoic rocks.

3.2. Hanging-wall faults of the Mosha Fault

The Taleqan Fault, located on the northern flank of the Taleqan Mountains, strikes E–W and dips to the south at 55°. The fault is the major hanging-wall fault of the Mosha Fault, and separates Paleozoic–Mesozoic rocks to the south from Tertiary rocks to the north (Fig. 4d,f). In addition to the Taleqan Fault, we also mapped, for the first time, a series of thrust sheets (TF1 to TF4 in Figs. 3, 4, 6) and thrust faults (TF5, TF6 in Figs. 3, 4, 6) in the hanging wall of the Mosha Fault. These sheets, with the exception of TF1, are only developed west of the Valian Valley (Fig. 3). The thrust sheets young toward the TF4 sheet (Table 1).

The TF1 thrust sheet is the oldest and structurally highest sheet in the hanging wall of the Mosha Fault, and comprises Precambrian rocks (Figs. 3, 4j). The base of the TF1 sheet is marked by several thrust faults that dip to the north at 50° (Fig. 4g). These thrust faults show a duplex geometry, with movement to the SW (Fig. 4h).

The TF2 thrust sheet, composed of Early Paleozoic rocks, strikes NW–SE and terminates against the Taleqan Fault to the west (Fig. 3). The orientations of striations on the basal thrust of the sheet, as observed along the section B–B′ (Figs. 3, 4e), indicate purely reverse movement upon the fault (Fig. 6a).

The TF3 thrust sheet comprises Late Paleozoic to Triassic formations (Fig. 3, Table 1). This sheet is the largest of those within the hanging wall of the Mosha Fault, and is best exposed along section B–B′ (Fig. 4b,c,e).

The TF4 thrust sheet strikes WNW–ESE, similar to the other sheets, and contains Jurassic rocks (Figs. 3, 4e, Table 1). The geometry of an overturned hanging-wall anticline demonstrates the shallow dip of the sheet (Fig. 7a,b). Extensive, minor asymmetric folds and S–C structures are observed at the base of the sheet within coal-bearing shale (Fig. 7c,d). These structures suggest movement of the sheet to the SW, indicating dextral reverse displacement (Fig. 6e).

The TF5 thrust strikes NW–SE and is located within the footwall of the TF2 sheet. The thrust is interpreted as a footwall imbricate thrust associated with the TF2 sheet (Figs. 3, 6). Extensive S–C structures are observed within the thrust zone, in which large

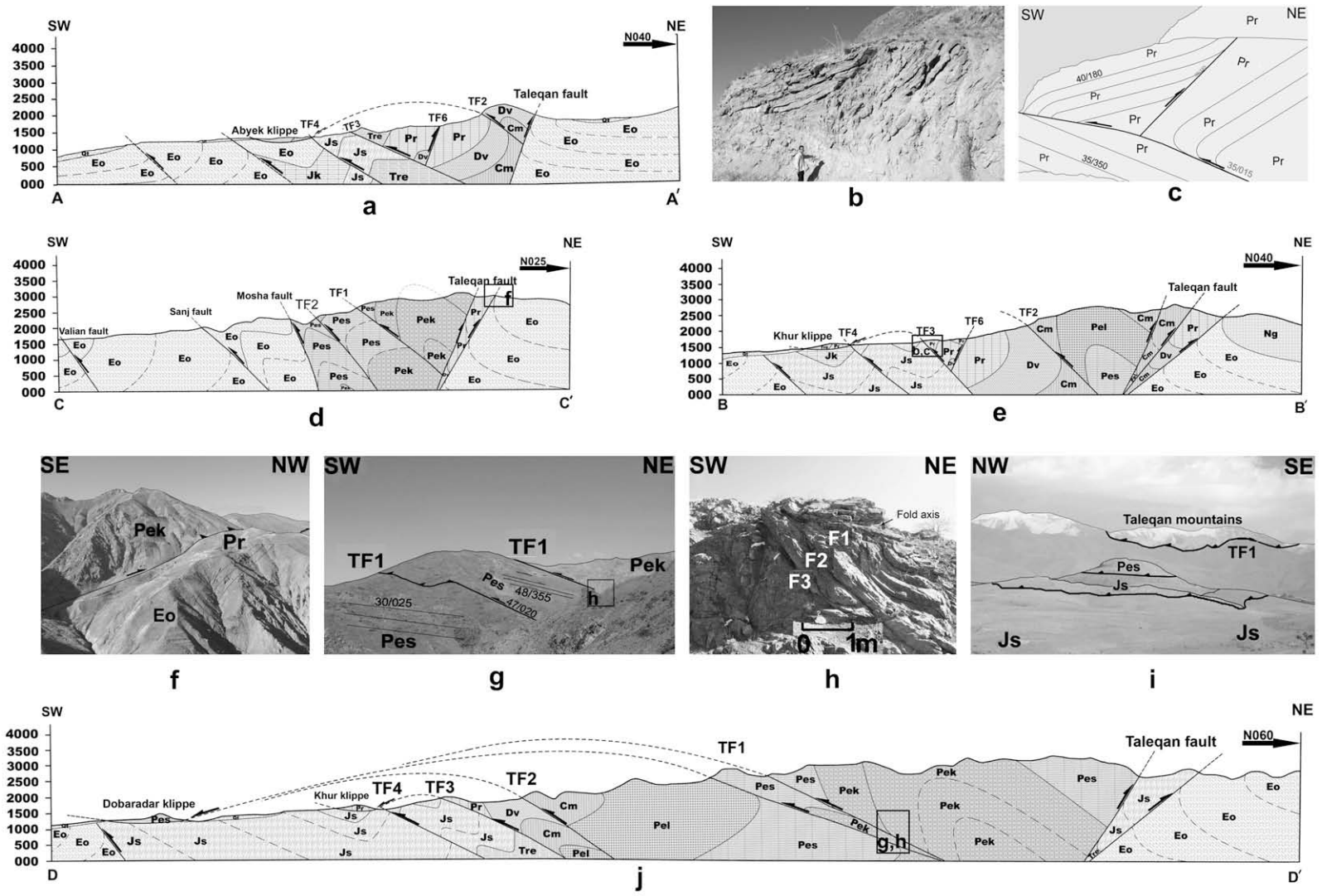

Fig. 4. (a) Structural section along A–A′ (see Fig. 3 for locations of cross-sections and legend). (b) Hanging-wall imbricate thrust associated with the TF3 fault, and back-thrust within Permian limestone. (c) Sketch map of (b). (d) and (e) Structural sections along C–C′ and B–B′, respectively. (f) Photograph of the Talegan Fault, showing the emplacement of Paleozoic rocks over Tertiary rocks. (g) Photograph of the TF1 thrust zone. (h) Thrust duplex system in the TF1 thrust zone, showing thrusting to the southwest. (i) Dobaradar Klippe upon the plains area located southwest of the Taleqan Mountains. Note the thrusting of Precambrian rocks over the Jurassic Shemshak Formation. For the location of the klippe, see section D–D′ in (j). (j) Structural section along D–D′.

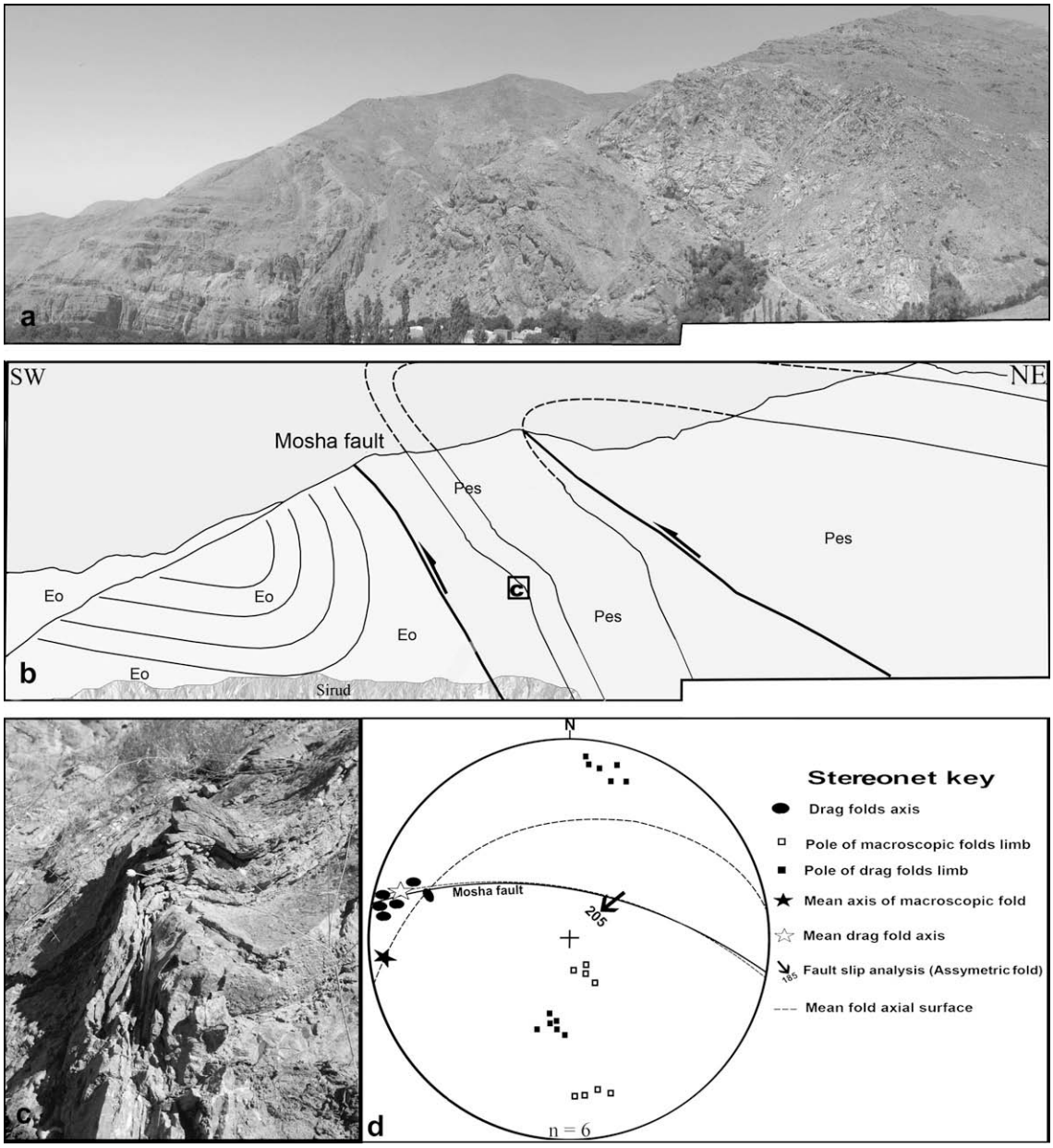

Fig. 5. (a) Photograph of the Mosha Fault in the eastern part of the Talegan Mountains, along cross-section C–C′. Note the development of a major hanging-wall anticline in Precambrian rocks and footwall syncline in Tertiary rocks. (b) Sketch map of (a) looking to the northwest. (c) Minor asymmetric folds in the Mosha Fault zone. (d) Stereonet showing the orientations of minor asymmetric fold axes (dots) and the intersection lineations between the fault plane and the fault zone foliation (dashed lines), demonstrating movement upon the Mosha Fault to the SW. Lower hemisphere, equal-area projection.

enclaves of Devonian volcanics are oriented along the S and C planes (Fig. 8a,b). The geometry of these planes indicates movement of the sheet to the SW (Fig. 6b).

The TF6 thrust fault dips at 60° to the south and occurs within the TF3 thrust sheet (Figs. 3, 4e). Asymmetric drag folds and S–C structures within the fault zone indicate movement to the NW (Fig. 6c).

3.3. Allochthonous masses

The plains area located southwest of the Taleqan Mountains contains several Precambrian–Triassic masses surrounded by younger, underlying Jurassic rocks (Figs. 3, 6). We mapped these masses in this study for the first time. These masses are lithologically similar to those of the thrust sheets, and are therefore interpreted to represent allochthons that originated from the overthrusting of sheets TF1–TF4 over the Jurassic rocks (Fig. 4, Table 1). From NW to SE, the main masses are the Sanghabad, Abyek, West Hive, Bajehband, Ghalegardan, Dobaradar, and Khur klippen (Fig. 6).

The Dobaradar and Ghalegardan klippen consist of Infra-Cambrian cherty dolomite, similar to the lithology of sheet TF1 (Table 1), and are thrust over the Jurassic Shemshak Formation (Fig. 4i). These klippen are therefore inferred to represent the TF1 sheet (Fig. 4j). The Abyek Klippe, the largest allochthonous mass in the study area, comprises Early Paleozoic rocks thrust over the Jurassic Shemshak Formation and Cretaceous carbonate rocks (Figs. 3, 6). The klippe is interpreted to represent the TF2 sheet based on lithologic similarity (Fig. 4a, Table 1). The Khur Klippe comprises Permian and Triassic rocks thrust over Jurassic rocks (Figs. 3, 6), and is correlated with the TF3 thrust sheet based on lithologic criteria (Fig. 4e, Table 1). Similarly, the Sanghabad, Bajehband, and West Hive klippen, comprising Permian carbonate rocks thrust over Jurassic carbonates, are correlated with the TF3 thrust sheet (Table 1).

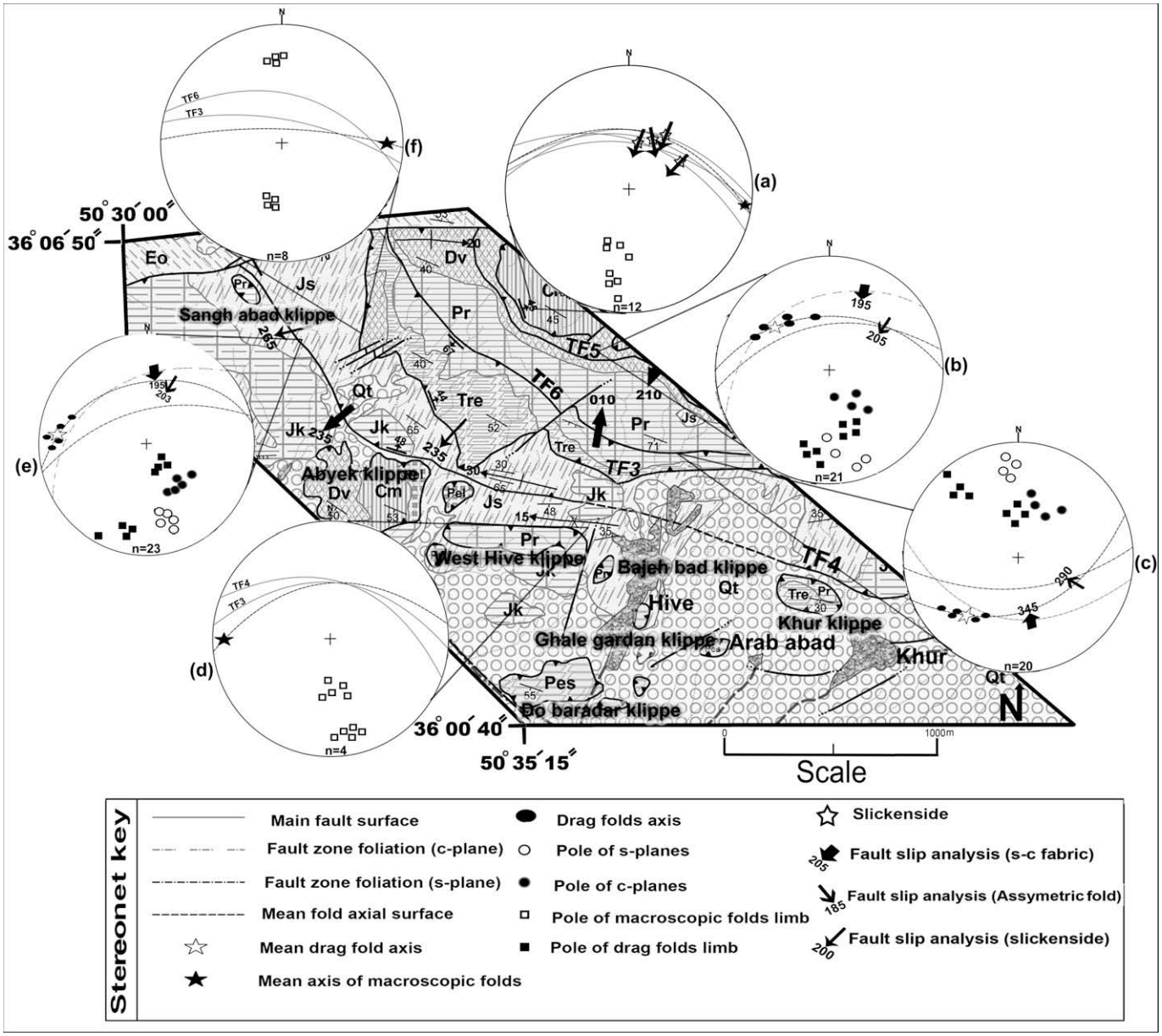

Fig. 6. Structural map of the allochthonous masses in the plains area located southwest of the Taleqan Mountains. Refer to Fig. 3 for the map location and legend. The stereonets represent (a) the movement direction of the TF2 thrust based on fault-plane striations; (b) the movement direction of the TF5 thrust based on the orientations of minor fold axes and S–C planes; (c) the movement direction of the TF6 thrust based on the orientations of minor fold axes and S–C structures; (d) the orientations of the TF3 and TF4 thrusts and axial surfaces of macroscopic folds; (e) the movement direction of the TF4 thrust based on the orientations of minor fold axes and S–C structures; and (f) the orientations of the TF3 and TF4 thrusts and axial surfaces of macroscopic folds.

3.4. Transverse faults

A set of N–S-striking faults cut transversely across the Mosha Fault and associated structures in the Taleqan Mountains. The most prominent transverse fault is located in the Valian Valley area (west of the C–C′ section line in Figs. 3, 9), marked by a distinct bend in the southern edge of the mountains and displacement of the Mosha Fault (Figs. 3, 9). The dip of the Mosha Fault decreases from east to west across the fault (compare Fig. 9d with e), and fold axes are curved in this area (Fig. 9).

A swarm of igneous dikes occurs within the Valian Valley area (Figs. 9, 10a), probably associated with granodioritic igneous bodies

Table 1
Characteristics of the allochthonous masses (klippen) located in the plains area southwest of the Talegan Mountains

Klippen (rock formations)	Original thrust sheets	Overthrust displacement in km	Estimated dip separation of thrust sheets in m
Dobaradar (Precambrian Soltanieh Formation)	TF1	18	3000
Ghalegardan (Precambrian Soltanieh Formation)	TF1	16	3000
Abyek (Early Paleozoic formations)	TF2	7	1800
Khur (Late Paleozoic-Triassic formations)	TF3	3	1000
Bajeband (Late Paleozoic formations)	TF3	2	1000
West Hive (Late Paleozoic–Triassic formations)	TF3	1.7	1000
Sanghabad (Late Paleozoic formations)	TF3	3.5	1000

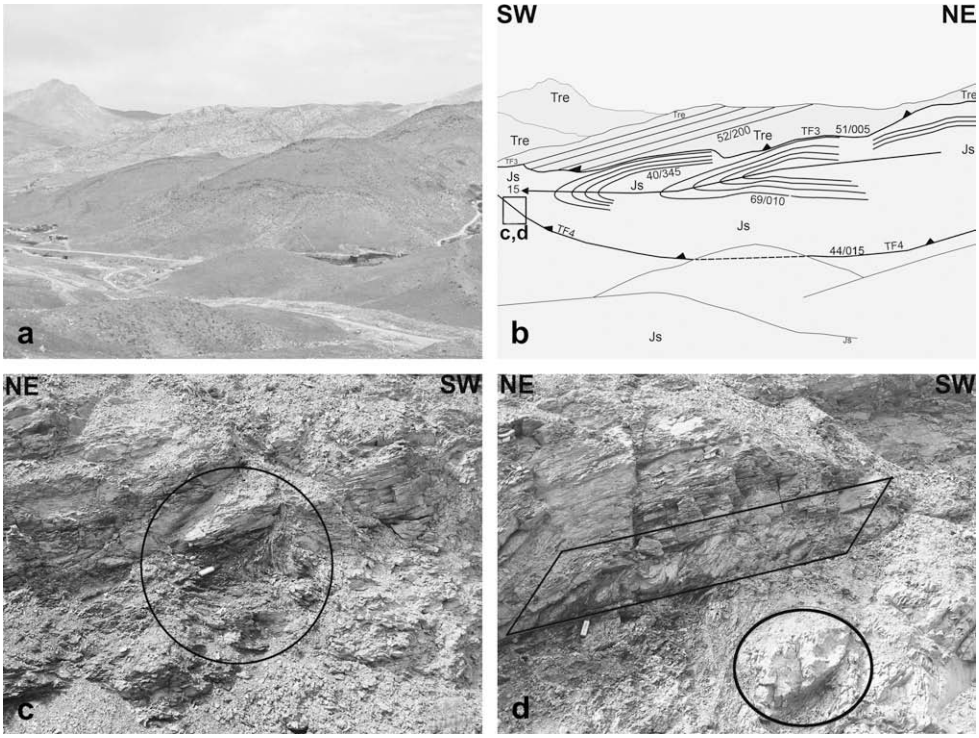

Fig. 7. (a) Photograph of the TF3 and TF4 thrust sheets. Note the development of an overturned anticline in the hanging wall of the TF4 thrust. (b) Sketch map of (a); (c) minor asymmetric folds in the TF4 thrust zone; (d) S–C structures in the TF4 thrust zone. Note the asymmetric boudinaged rocks within the fault zone.

exposed to the north-northwest (Fig. 3). Precambrian carbonate rocks are folded at the contact zone with the dikes (Fig. 10b), with the axial surfaces of the folds being oriented sub-parallel to the dikes (Fig. 10c), possibly indicating that folding was associated with intrusion. Similarly, the intrusion of igneous sills into Cambrian sandstone led to displacement along bedding planes (Fig. 10d). The direction of slip indicated by bedding-plane striations is consistent with the intrusion direction of the sills (Fig. 10e). The slip surfaces also show evidence of hydrothermal mineralization associated with fluids derived from the intrusive body.

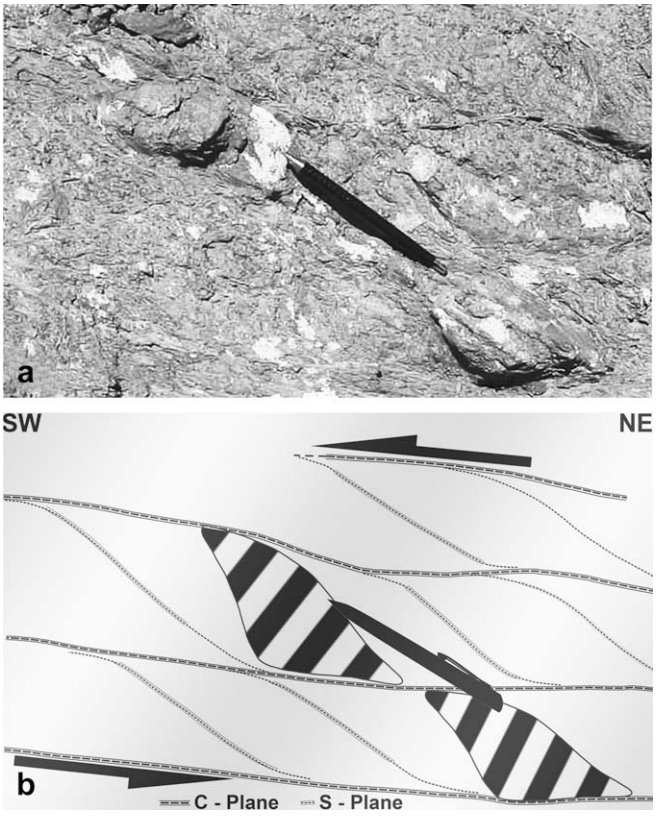

Fig. 8. (a) The TF5 thrust zone, showing top-to-the-SW thrusting. (b) Sketch map of (a). Note the development of S (fault-zone foliation) and C (shear plane) planes.

4. Discussion

4.1. Kinematics of the Mosha Fault

The Mosha Fault defines the southern margin of a Paleozoic–Mesozoic basin in the Central Alborz Range. The fault is considered to have acted as a basin-bounding fault since the Paleozoic. The hanging wall of the fault (i.e., to the north of the fault) was a suitable site for the deposition of Mesozoic carbonates. The dip of the fault is considered to reflect its origin as a normal fault subsequently reactivated as a reverse fault. This process has been demonstrated by McClay and Buchanan (1992) using a number of experimental models, in which pre-existing extensional faults were reactivated as high-angle reverse faults.

A detailed microstructural analysis of quartz-rich sandstone from the Mosha Fault zone in the eastern part of the study area demonstrated that deformation occurred under semi-ductile conditions (Moinabadi and Yassaghi, 2007). In the present study, analysis of structures associated with the Mosha Fault (i.e., a large-scale basement-cored hanging-wall anticline comprising Precambrian rocks, and a footwall syncline comprising Tertiary rocks; Fig. 5) reveals that the Mosha Fault is deep-seated and records a significant amount of displacement. The occurrence of a basement-cored hanging-wall anticline bounded by an inverted normal fault is a common feature of thick-skinned inverted normal faults (Tavarnelli et al., 2004).

The timing of inversion of the Mosha Fault has yet to be constrained in detail (Moinabadi and Yassaghi, 2007); however, a Late Mesozoic timing is indicated by the spatial distribution of Late

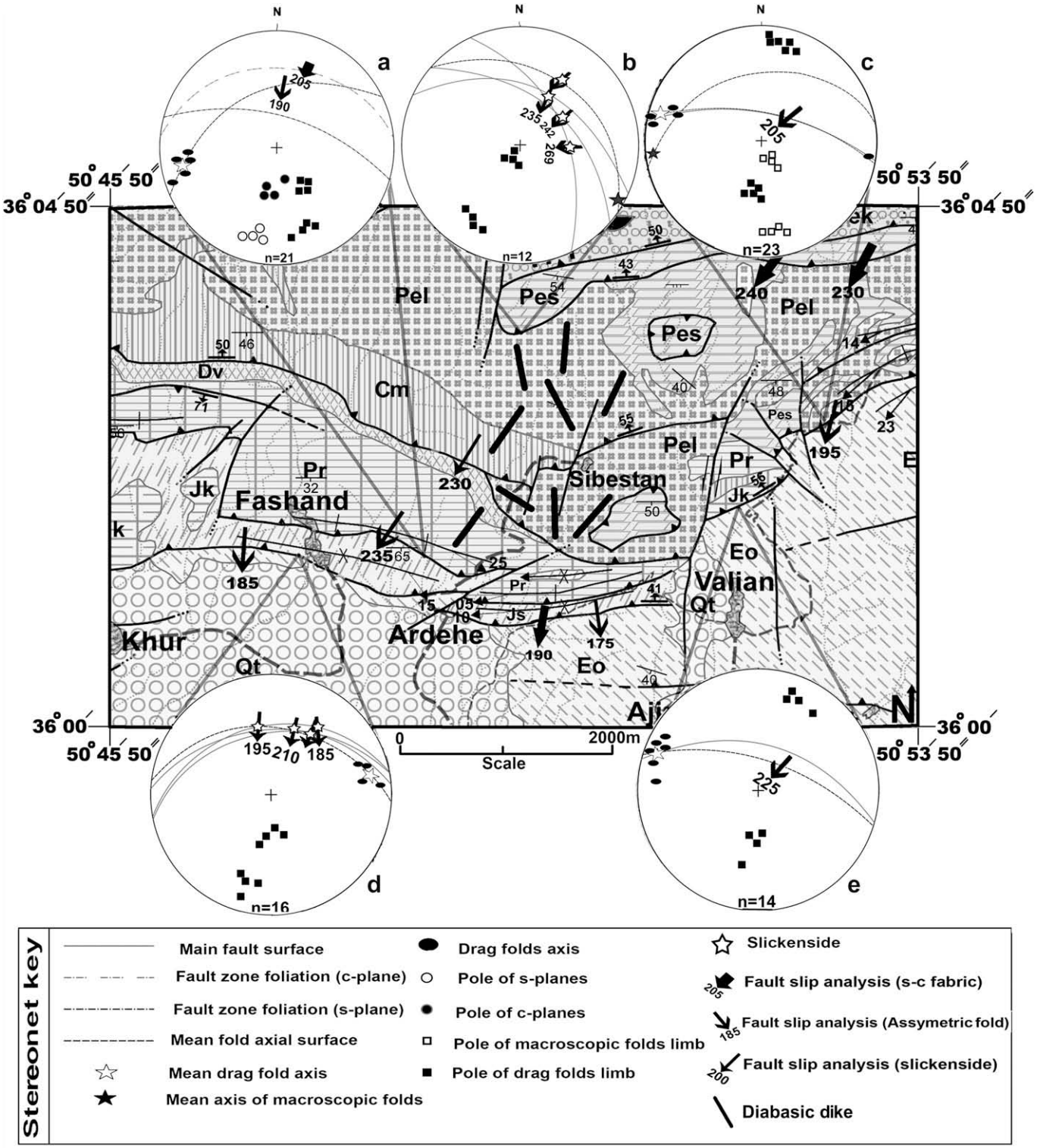

Fig. 9. Structural map of the Valian Valley. Note the displacement of the Mosha Fault to the south where it crosses the valley, and the location of a swarm of igneous dikes in the western part of the valley. Refer to Fig. 3 for the map location and legend. The stereonets represent analyses of the movement directions of the following faults: (a) the TF3 thrust based on the geometry of asymmetric minor folds and S–C structures lanes; (b) TF1 based on fault-plane striations; (c) the Mosha Fault east of the Valian Valley based on the geometry of asymmetric minor folds; (d) the Mosha Fault west of the Valian Valley based on the geometry of asymmetric minor folds and fault striations; and (e) the Mosha Fault east of the valley based on asymmetric minor folds.

Mesozoic pelagic carbonates (Sadeghi, 1999) in the hanging wall of the fault (i.e., the downthrown side of the normal fault), and the disconformable deposition of the Eocene Karaj tuff over the Early Mesozoic sediments of the footwall (Figs. 3, 4).

The eastern portion of the Mosha Fault has been interpreted as a left-lateral strike-slip fault with 30–35 km of horizontal displacement (Allen et al., 2003), whereas the central part of the fault has been interpreted as a reverse fault (Moinabadi and

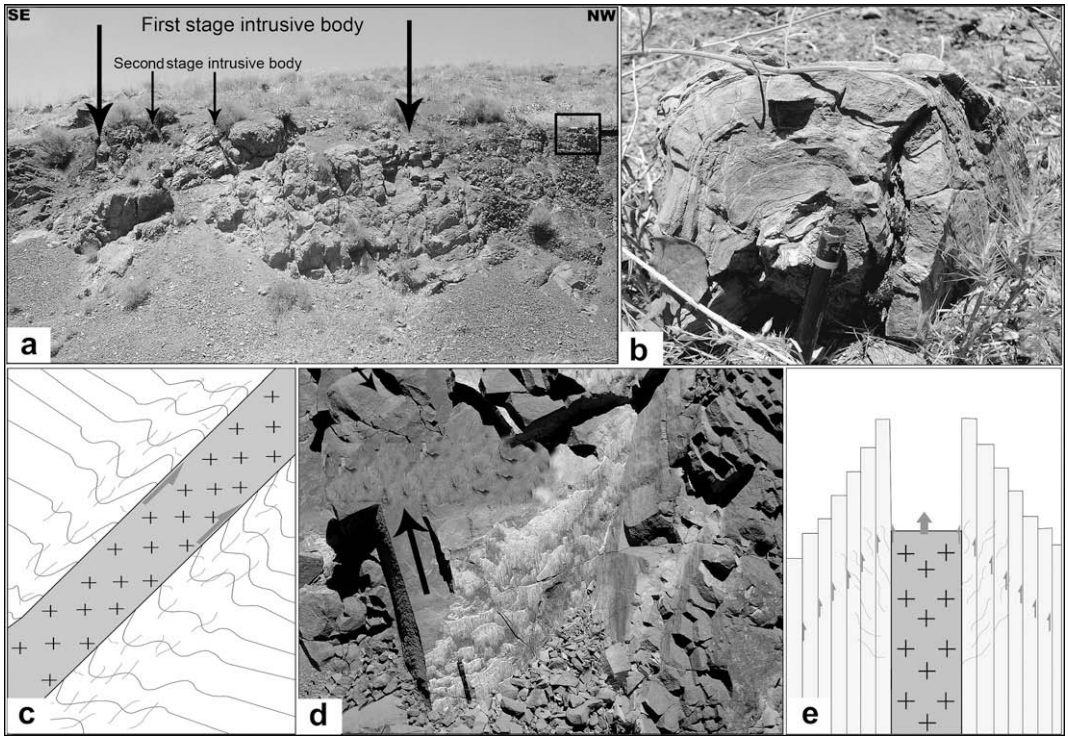

Fig. 10. Igneous dikes and associated structures along the Valian Valley. (a) Two stages of dike intrusion. (b) Development of minor folds in Precambrian carbonate host rocks. (c) Sketch map of an intrusive dike and minor folds in the host rocks. (d) Intrusive sills within Cambrian sandstone rocks in which slip lines (arrow) are developed on bedding surfaces. (e) Sketch showing the development of slip lines within the host sandstone during intrusion of the sills.

Yassaghi, 2007). In the present study area (i.e., western portion of the fault, in the Taleqan Mountains), the orientations of striations upon the fault plane and geometries of S–C structures and minor asymmetric folds indicate reverse movement (western parts of the Valian Valley, Fig. 9d) or reverse movement with a minor left-lateral strike-slip component (eastern parts of the Valian Valley, Fig. 9e).

Allochthonous masses in the plains area to the south of the Taleqan Mountains (Figs. 3, 6) mainly originated from the TF1, TF2, and TF3 thrust sheets located in the hanging wall of the western-most part of the Mosha Fault. The distances between each of these masses and their source thrust sheets decrease from TF1 to TF3 (Table 1), demonstrating that the thrusting occurred in sequence, from the older TF1 sheet to the younger TF4 sheet, toward the southwest. The amount of dip-slip separation between each thrust sheet is less than the surface distance between the thrust sheets and corresponding allochthonous masses (Fig. 4, Table 1). We propose that ramping of the younger thrust sheets caused passive uplift of the older thrust sheets to higher structural levels, resulting in the allochthonous masses being transported greater distances. This ramping process also resulted in greater gravitational sliding for the older thrust sheets. A similar process has been proposed for the central Pyrenees (Saura and Teixell, 2006). The TF5 thrust is inferred to represent a footwall-connecting branch to the TF2 thrust, and the TF6 thrust as a back-thrust to the TF3 thrust (Fig. 4).

4.2. Along-strike variations in the geometry of the Mosha Fault

The inversion of high-angle normal faults is usually accommodated in the fault footwall by shortcut thrusts (Buchanan and McClay, 1991). Such shortcut thrusts within the footwall of the Mosha Fault have been mapped to the east of the present study area (Moinabadi and Yassaghi, 2007). The Taleqan Mountains represent a pop-up structure of Paleozoic–Mesozoic rocks, bounded by the steeply north-dipping Mosha Fault and south-dipping Taleqan Fault (Figs. 3, 4d). Consequently, the Taleqan Fault is considered likely to rejoin the main fault at depth, thereby leading to the exposure of older rocks in a pop-up structure (Fig. 3). The Taleqan Fault is therefore interpreted as a back-thrust to the Mosha Fault. This structural geometry, prominent in the eastern part of the study area (east of the Valian Valley; Figs. 3, 9), is similar to that proposed for inverted normal faults in which basement is involved during inversion (McClay and Buchnan, 1992; Coward, 1994; Tavarnelli et al., 2004). In the western part of the study area, the Mosha Fault is relatively shallow, with no evidence of footwall shortcut thrusts; instead, we observes a series of thrust sheets in the form of hanging-wall break-back bypass thrusts (Figs. 3, 4) (e.g., Coward, 1994).

Coward (1994) reported along-strike variations in the geometry of inverted normal faults in the Pyrenees, from footwall shortcut thrusts to hanging-wall break-back thrusts. Footwall shortcut thrusts develop during the reactivation of high-angle normal faults. In the case of low-angle normal faults, however, deformation is transferred to the hanging wall as thin-skinned thrust sheets detached at a structural level above basement. In the eastern part of the Taleqan Mountains, the Mosha Fault is a high-angle reactivated thrust fault (Moinabadi and Yassaghi, 2007). The presence of the Precambrian Kahar Formation in the hanging wall in this part of the study area (Fig. 3) implies basement involvement in thrusting (e.g., Mitra and Mount, 1998). In the western part of the study area (west of the Valian Valley), however, the shallower dip of the Mosha Fault, in combination with its roll-over geometry, led to the development of thin-skinned thrust sheets (TF1–TF4 in Figs. 3, 8).

Extensive structural data from the Valian Valley indicate the existence of a major deep-seated transverse fault that passes through the valley and/or crosses the Central Alborz Range. Evidence for the fault includes the spatial distribution of intrusive igneous bodies within Precambrian–Cambrian rocks and the development of deformation structures along their contacts (Figs. 9, 10), the truncation and displacement of thrust faults, and

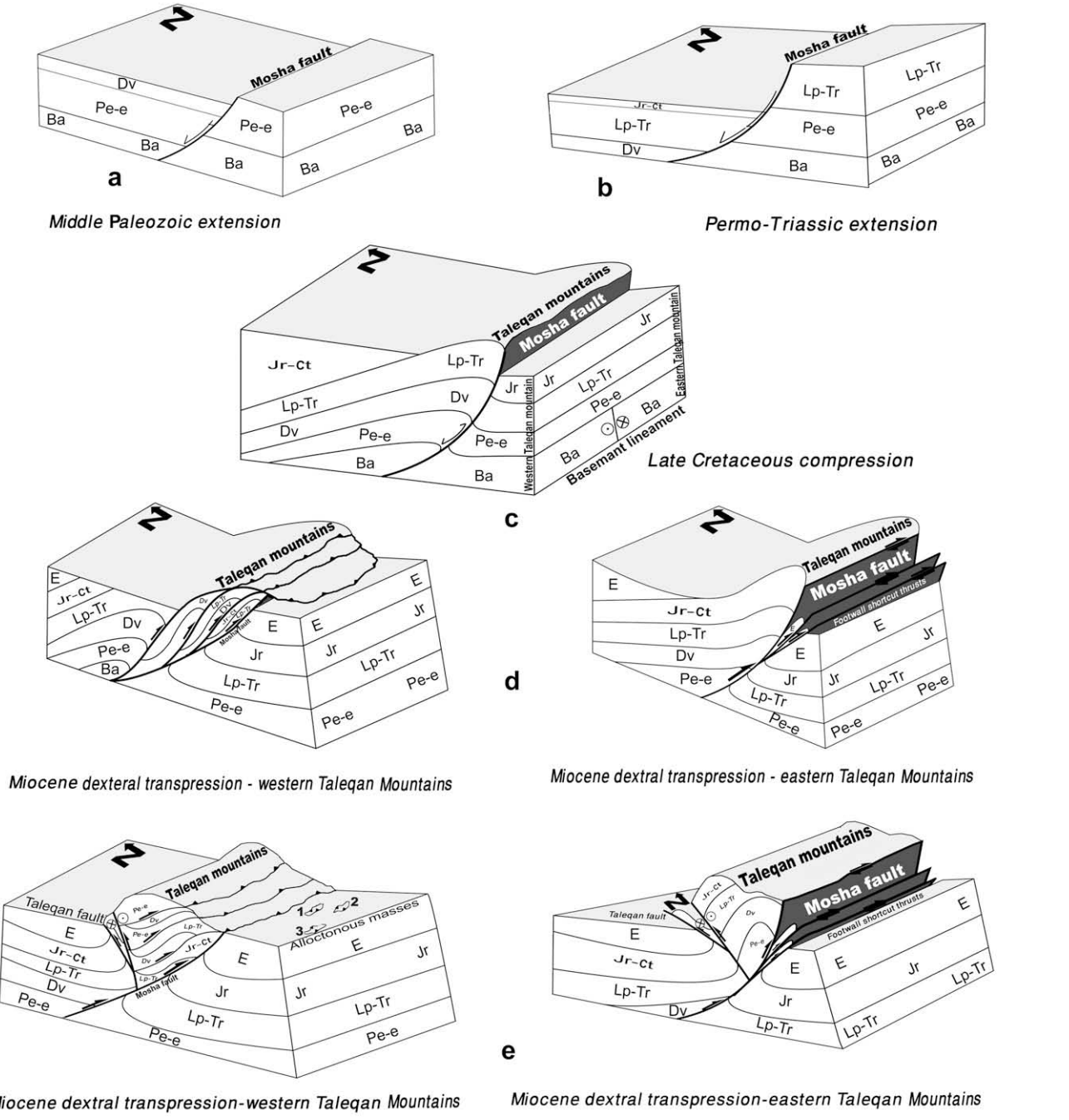

Fig. 11. Structural model proposed for the development of the Mosha Fault from an initial extensional stage during the Paleozoic to the final compressional stage during the Late Tertiary. See text for details. The numbers in (e) represent allochthonous masses related to the TF1, TF2, and TF3 thrust sheets. The location of the eastern and western parts of the Taleqan Mountains is presented in Fig. 12. Abbreviations: Ba, Basement; Pe-e, Precambrian–Silurian; Dv, Devonian; Lp-Tr, Early Paleozoic–Triassic; Jr-Kt, Jurassic–Cretaceous; E, Tertiary.

the curvature of fold axial traces for which the orientations of fold axes differ from those of the axial traces (Fig. 9). In addition, the Mosha Fault shows an along-strike variation in geometry across the Valian Valley. We therefore propose that the Valian Valley marks the location of a basement fault, herein named the Valian Basement Fault, active since at least the Mesozoic. The effects of the Valian Basement Fault can be traced northwest to the Alam Kuh intrusive igneous body on the southern coast of the Caspian Sea (Fig. 2).

The influence of transverse basement faults on along-strike variations in the dip angle of reactivated normal faults has also been reported in the Apennines and French Alps (Castellarin et al., 1982; Gillcrist et al., 1987; Tavarnelli et al., 2004), where high heat flow and igneous activity are also associated with the basement faults (Butler et al., 2006). Similarly, in the Zagros fold belt of Iran (see inset map in Fig. 2), where the basement rocks are similar to those of the Alborz Range (Stöcklin, 1968), the development of curved fold axial traces is interpreted to reflect the influence of basement faults on the cover sequence (Hessami et al., 2001; Yassaghi, 2006).

4.3. Structural model of the Taleqan Mountains

The Taleqan Mountains comprise a Paleozoic–Late Tertiary succession, with a thick sequence of Early Paleozoic volcanics that

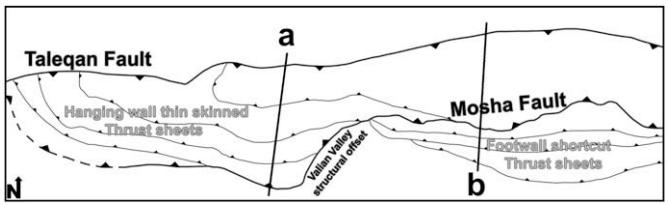

Fig. 12. Sketch map of the structure of the Talegan Mountains, showing the distribution of footwall shortcut thrusts associated with the Mosha Fault (eastern side of the Valian Valley) and hanging-wall break-back thrusts associated with the Mosha Fault (western side of the valley). Block diagrams for the section lines a and b are presented in Fig. 11.

includes basal pillow lava that represents the initiation of rifting (Fig. 11a) (e.g., Stöcklin, 1968; Guest et al., 2006). The volcanic sequence is conformably overlain by a Late Devonian–Triassic succession, possibly indicating continuation of the extensional phase until the Late Triassic (Fig. 11b).

The influence of the Cimmerian Orogeny on the Central Alborz Range involved the peripheral bulging of faults and/or continuation of their extensional movement (Zanchi et al., 2006). The process of swell and sag along normal faults (e.g., the Mosha Fault) is interpreted to be controlled by transverse basement faults such as the Valian Basement Fault. The deposition of a greater thickness of Late Mesozoic marine carbonates in the hanging wall of the Mosha Fault to the west of the Valian Basement Fault (compared with the east) indicates a greater degree of sagging along the western segment. This also indicates the development of sag and swell topography in the hanging wall of the Mosha Fault on both sides of the Valian Basement Fault during the Late Mesozoic.

Reactivation of the Mosha Fault as a reverse fault is interpreted to have been initiated by the Late Cretaceous (Section 4.1 and Figs. 4, 11c). This compressional phase began with the arc–continent collision stage of the Zagros orogeny (Mohajjel et al., 2003). Late Miocene continent–continent collision between the African–Arabian Plate and the Iranian microcontinent (Berberian and King, 1981) led to right-lateral transpression in the Alborz Range (Axen et al., 2001; Allen et al., 2003). This collisional event saw the development of footwall shortcut thrusts in the eastern part of the study area (central Mosha Fault; Moinabadi and Yassaghi, 2007) and hanging-wall break-back thrust sheets in the western part of the study area (Figs. 9, 11d, 12). Similarly, the Taleqan Fault developed as a back-thrust to the Mosha Fault during continuing inversion of the Mosha Fault (Fig. 11e). Movement upon the back-thrust led to the exposure of older rocks in a pop-up structure (Fig. 11e), triggering in turn the passive movement of thrust sheets to structurally higher levels, accompanied by the emplacement of allochthonous masses as klippen upon the plains to the southwest of the mountains (Nos. 1–3 in Fig. 11e).

5. Conclusion

The NW-trending Mosha Fault is a basin-bounding fault that separates Tertiary rocks in the footwall (southern side of the fault) from Precambrian–Mesozoic rocks in the hanging wall (northern side). Thick-skinned inversion upon the Mosha Fault in the eastern part of the Taleqan Mountains is indicated by the steep dip of the fault, the development of a large basement-cored hanging-wall anticline, and footwall synclines and/or shortcut thrusts. In the western part of the Taleqan Mountains, the Mosha Fault dips at a lower angle than that in the east, and is associated with thin-skinned break-back thrust sheets in the hanging wall. The strata exposed on the eastern side of the Valian Valley represent a mainly Precambrian to Early Paleozoic platform succession, while the western side of the valley consists of Mesozoic marine carbonates. Along-strike variations in the geometry of the Mosha Fault that occur across the Valian Valley are inferred to be related to a steeply dipping NNE–SSW-striking basement transfer fault oriented at a high angle to the strike of the Mosha Fault. This transverse basement fault controls the distribution of dispersed igneous intrusives, the curvature of fold axes, and discontinuities in regional fault trends across the valley.

Acknowledgements

This study was supported by Tarbiat Modares University, Tehran. We thank Chris Fergusson and an anonymous reviewer for their reviews and helpful suggestions.

References

Alavi, M., 1996. Tectonostratigraphic synthesis and structural style of the Alborz mountain system in northern Iran. Journal of Geodynamics 21, 1–33.
Allen, M.B., Ghassemi, M.R., Shahrabi, M., Qorashi, M., 2003. Accommodation of late Cenozoic oblique shortening in the Alborz range, northern Iran. Journal of Structural Geology 25, 659–672.
Ashtari, M., Hatzfeld, D., Kamalian, N., 2005. Microseismicity in the region of Tehran. Tectonophysics 395, 193–208.
Axen, G.J., Lam, P.J., Grove, M., Stockli, D.F., Hassanzadeh, J., 2001. Exhumation of the west-central Alborz Mountains, Iran, Caspian subsidence, and collision-related tectonics. Geology 29, 559–562.
Berberian, M., King, G.C.P., 1981. Towards the paleogeography and tectonic evolution of Iran. Canadian Journal of Earth Sciences 18, 210–265.
Berberian, M., Qorashi, M., Argang Ravesh, B., Mohajer Ashjaie, A., 1993. Seismotectonic and earthquake-fault hazard investigation in the Tehran Region, contribution to the seismotectonic of Iran, part V, Report No 56. Geological Survey of Iran.
Brooks, M., Llewelyn, D.J., Mechie, J., 1983. Geophysical investigations in the Variscides of southwest Britain. In: Hancock, P.L. (Ed.), The Variscan Fold Belt in the British Isles. Adam Hilger, Bristol, pp. 186–197.
Buchanan, P.G., McClay, K.R., 1991. Sandbox experiments of inverted listric and planar faults systems. In: Cobbold (Ed.), Experimental and Numerical Modeling of Continental Deformation. Tectonophysics, 188, pp. 97–115.
Butler, R.W.H., Tavarnelli, E., Grasso, M., 2006. Structural inheritance in mountain belts: an Alpine-Apennine perspective. Journal of Structural Geology 28, 1893–1908.
Castellarin, A., Colacicchi, R., Praturlon, A., Cantelli, C., 1982. The Jurassic-lower Pliocene history of the Aneona-Anzio line (Central Italy). Memorie Della Socita Geologica Italiana 24, 325–336.
Coward, M., 1994. Inversion tectonics. In: Hancock, P. (Ed.), Continental Deformation. Pergamon Press, p. 421.
Dellenbach, J., 1964. Contribution a l'etude geologique de la region situee an l'est Teheran (Iran). Faculty of Science. University of Strasburg.
Etheridge, M.A., 1986. Major crustal lineaments and their influence on the geological history of continental lithosphere. Philosophical Transactions of the Royal Society of London. Series A. Mathematical and Physical Sciences 317, 179–194.
Gillcrist, R., Coward, M., Mugnier, J., 1987. Structural inversion and its controls: examples from the Alpine foreland and French Alps. Geodinamica Acta 1, 5–34.
Guest, B., Axen, G.J., Lam, P.S., Hassanzadeh, J., 2006. Late Cenozoic shortening in the west-central Alborz Mountain, northern Iran, by combined conjugate strike slip and thin-skinned deformation. Geosphere 2, 35–52.
Hayward, A.B., Graham, R.H., 1989. Some geometrical characteristics of inversion. In: Cooper, M.A., Williams, G.D. (Eds.), Inversion Tectonics, 44. Geological Society Special Publication, pp. 17–39.
Hessami, K., Koyi, H.A., Talbot, C.J., 2001. The significance of strike slip faulting in the basement of the Zagros fold and thrust belt. Journal of Petroleum Geology 24, 5–28.
Konstantinovskaya, E.A., Harrisa, L.B., Poulina, J., Ivanova, G.M., 2007. Transfer zones and fault reactivation in inverted rift basins: Insights from physical modeling. Tectonophysics 441, 1–26.
Koopman, A., Specksnijder, A., Horsfield, W.T., 1987. Sand box studies of inversion Tectonics. Tectonophysics 137, 379–388.
Lasemi, Y., 2000. Facieses, sedimentary environment and sequence stratigraphy of Upper-Precambrian and Paleozoic rocks of Iran. 18th Symposium of Earth Sciences. Geological Survey of Iran.
McClay, K.R., Buchanan, P.G., 1992. Thrust faults in inverted extensional basins. In: McClay, K.R. (Ed.), Thrust Tectonics. Chapman and Hall, London, pp. 93–104.
Mitra, S., Mount, V.S., 1998. Foreland basement involved structures. American Association of Petroleum Geologists Bulletin 82, 70–109.
Mohajjel, M., Fergusson, C.L., Sahandi, M.R., 2003. Cretaceous-Tertiary convergence and continental collision, Sanandaj-Sirjan zone, western Iran. Journal of Asian Earth Sciences 21, 397–412.
Moinabadi, M.E., Yassaghi, A., 2007. Gemometry and kinematics of the Mosha fault, south Central Alborz Range, Iran: An example of basement involved thrusting. Journal of Asian Earth Science 29, 928–938.

Powell, C.M., 1989. Structural controls on Paleozoic basin evolution and inversion in southwest Wales. Journal of Geophysical Society London 146, 439–446.

Quintana, L., Alonso, J.L., Pulgar, J.A., Rodriguez-Fernandez, L.R., 2006. Transpressional inversion in an extentional transfer zone (the Saltacaballos fault, northern Spain). Journal of Structural Geology 28, 2038–2048.

Sadeghi, A., 1999. Assessment of Cretaceous deposits in southern slopes of Central Alborz. PhD thesis, Shahid Beheshti University.

Saura, E., Teixell, A., 2006. Inversion of small basins: effects on structural variations at the leading edge of the Axial Zone antiformal stack (Southern Pyrenees, Spain). Journal of Structural Geology 28, 1909–1920.

Stöcklin, J., 1968. Structural history and tectonics of Iran: a review. American Association of Petroleum Geologists Bulletin 52, 1229–1258.

Stöcklin, J., 1974. Mesozoic-Cenozoic Orogenic Belts: Data for Orogenic Studies. In: Spencer, A. (Ed.), Northern Iran: Alborz Mountains, 4. Geological Society Special Publication, London, pp. 213–234.

Stockmal, G.S., Slingsby, A., Waldron, J.W.F., 2004. Basement-involved inversion at the Appalachian structural front, western Newfoundland: an interpretation of seismic reflection data with implications for petroleum prospectivity. Bulletin of Canadian Petroleum Geology 52, 215–233.

Tavarnelli, E., Butler, R.W.H., Decandia, F.A., Calamita, F., Grasso, M., Alvarez, W., Rena, P., 2004. Implications of fault reactivation and structural inheritance in the Cenozoic tectonic evolution of Italy. In: Cressenti, U., D'Offizi, S., Merlini, S., Sacchi, R. (Eds.), The Geology of Italy, Special Volume I. Societa Geologica Italiana, pp. 209–222.

Vahdati Daneshmand, F., 2001. Geological map of Marzan Abad, Geological Survey of Iran. Quadrangle map. Scale 1, 100000.

Ventisette, C.D., Montanari, D., Sani, F., Bonini, M., 2006. Basin inversion and fault reactivation in laboratory experiments. Journal of Structural Geology 28, 2067–2083.

Williams, G.D., Powell, C.M., Cooper, M.A., 1989. Geometry and kinematics of inversion Tectonics. In: Cooper, M.A., Williams, G.D. (Eds.), Inversion Tectonics, 44. Geological Society Special Publication, pp. 3–15.

Yassaghi, A., 2001. Inversion tectonics in the Central Alborz Range. European Union of Geosciences (EUG XI), 335. Abstract. Symposium LS05.

Yassaghi, A., 2006. Integration of Landsat imagery interpretation and geomagnetic data on verification of deep-seated transverse fault lineaments in SE Zagros. International Journal of Remote Sensing 27, 4529–4544.

Zanchi, A., Berra, F., Mattei, M., Ghassemi, M.R., Sabouri, J., 2006. Inversion tectonics in central Alborz, Iran. Journal of Structural Geology 28, 2023–2037.